Optimization of turbine start-up sequence of a full size frequency converter variable speed pump-turbine

Optimization of turbine start-up sequence of a full size frequency converter variable speed pump-turbine

J Schmid[1], S Alligné[1], D Biner[2,3], C Münch-Alligné[2], N Hugo[4], C Nicolet[1]

[1] Power Vision Engineering Sàrl, St-Sulpice, Switzerland
[2] Institute of Systems Engineering, School of Engineering, HES-SO Valais-Wallis, Rue de l'Industrie 23, Sion, Switzerland
[3] Power Electronics Laboratory – PEL, Ecole Polytechnique Fédérale de Lausanne, Lausanne, Switzerland
[4] Alpiq SA, Lausanne, Switzerland

E-Mail: jeremy.schmid@powervision-eng.ch

Abstract. The stability of the electricity grid will be disrupted by the massive integration of new renewable energies. Hydropower plants have a major role to play in this transformation of the electricity market by increasing their operational flexibility and their ability to provide ancillary services. However, this flexibility may lead to an accelerated degradation of mechanical components. By changing the turbine operating point far from the best efficiency point or by increasing the number of transient manoeuvres such as start and stop sequences, unsteady flow phenomena, cavitation development and additional wear and tear stress the unit's components and impact its lifetime. The present work aims to provide preliminary insight on the optimization of the start-up sequence of a 5 MW reversible Francis pump-turbine equipped with a Full Size Frequency Converter (FSFC). The goal of the optimization approaches are to determine a start-up sequence which minimizes the runner damage, the penstock fatigue and the water losses. The objective functions are evaluated by 1D hydraulic transient simulations with the SIMSEN software and which it allow to compare the relative mitigation between the conventional fixed-speed start-up and the linear variable-speed start-up equipped with a Full Size Frequency Converter.

1. Introduction

To achieve the European Union's CO2 emission targets by 2050, the structure of the power supply system will change considerably due to the massive arrival of variable renewable energy (VRE) [1]. VREs are being deployed on a large scale to enable electrification based on clean and low-carbon energy. Furthermore, these VREs are stochastic and non-dispatchable in nature, which implies constraints and challenges to be solved for the proper functioning of the power supply system. The XFLEX HYDRO H2020 European Project aims to demonstrate, with new technologies, the control and flexibility capabilities of the hydropower plants and, consequently, their key role in future electricity supply system [1]. These new technologies currently under study in this project such as smart control, variable speed hydraulic units [2], hydraulic short circuit, and battery-turbine hybridization aim to be demonstrated to improve the power grid stabilization. In the XFLEX HYDRO project, there are seven European hydropower plant demonstrators that provide experimental data to assess the advantages and limits of these technologies. The Z'Mutt pumping station, located in Zermatt, Switzerland, part of the Grande Dixence development, supplying the main adduction of the Lac des Dix, has been chosen as one of the demonstrators. A new 5 MW reversible Francis pump-turbine, currently being installed in 2022, is equipped with a Full Size Frequency Converter, FSFC.

The targeted control capacities and operating flexibilities of hydropower units may lead to accelerated degradation of hydromechanical components which results from increase number of start-up and stop cycles, by moving the operating point far from the best efficiency point (BEP), and even transition from pumping mode to turbine mode [3], [4]. These frequent transient sequences may induce critical phenomena, such as cavitation effect and unsteady pressure fields causing stresses and wears on mechanical components, impacting their lifetime [5]. To avoid premature fatigue, the optimisation process for the Z'Mutt pumping station is performed using several stages and inputs such as model tests performing by the EPFL Technology Platform for Hydraulic Machines, detailed CFD and FEM analysis of the prototype to map the damage rate of the runner performed by HES-SO Valais-Wallis, and 1D transient hydroelectric simulations performed by Power Vision Engineering. All these results will be integrated into the unit controller in order to optimize the unit lifetime.

The paper presents a single and multi-objective optimization of the transient start-up sequence of the Z'Mutt Francis pump-turbine equipped with FSFC. The FSFC technology allows to avoid a fixed-speed start-up passing through the speed-no-load operation (SNL), thanks to the power converter able to decouple the frequency between the grid and the generator. A previous study has demonstrated that the speed controller is more preferable for the unit stability than the power controller. Therefore, in this case, the speed controller is used to perform start-up control, see [6], [8]. The single and multi-objective optimisation of the start-up sequence by means of 1D transient simulation aim to consider the efficiency BEP tracking, the runner damage and the fatigue on the penstock. The optimisation process is performed using algorithms from the MATLAB commercial tool called Global Optimisation toolbox [13] and the results are compared to the conventional fixed-speed start-up and the linear variable-speed start-up.

2. Z'Mutt power plant demonstrator

Z'Mutt is a Pumping Station (PS) located in Zermatt, Switzerland. Z'Mutt PS, schematized in Figure 1, is the largest pumping station of the Grande Dixence hydroelectric scheme. This pumping station is equipped with two 30 MW pump units (U1, U2), two 14 MW pump units (U3, U4) and finally one 5 MW reversible pump-turbine unit (U5). The new unit U5, which is the scope of the study, is equipped with an asynchronous motor-generator, driven by a FSFC. The pump-turbine is characterized by a specific speed of Nq = 54 and a unit mechanical time constant of τ_m=1.3 s. The main hydraulic characteristics are given in Table 1.

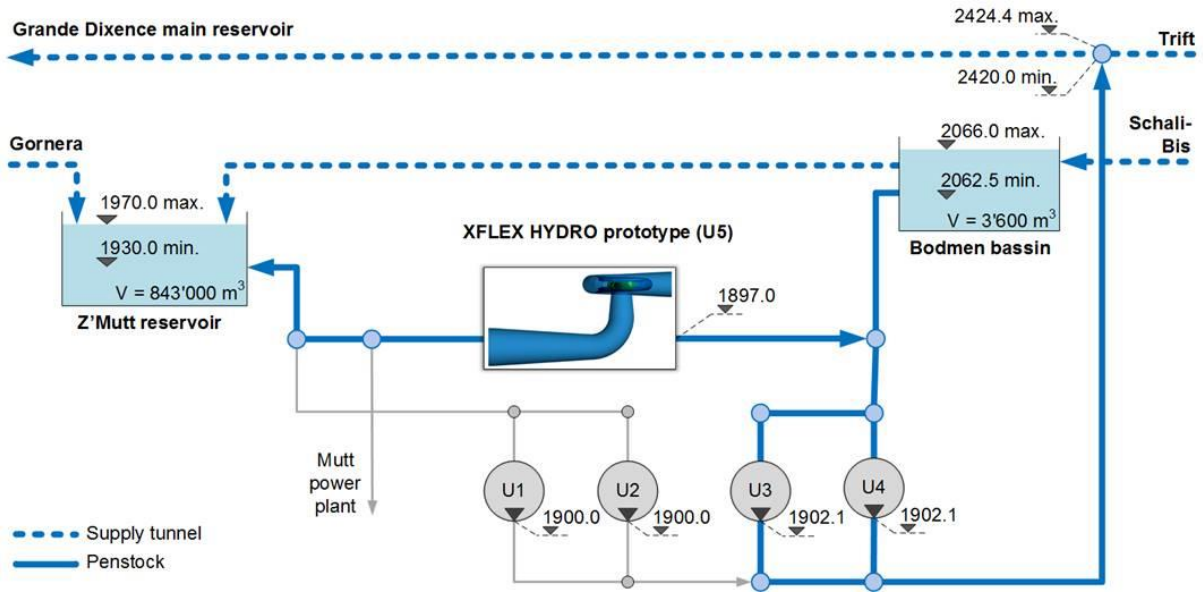

Figure 1: Schematic of the Z'Mutt pumping station.

Table 1: Hydraulic and mechanical characteristics of unit U5 in pump mode.

Data		Unit	Value
Nominal flow rate	Qn	$m^3 \cdot s^{-1}$	3.6
Nominal head	Hn	mWC	115
Nominal rotational speed	Nn	min^{-1}	1000
Diameter of reference	Dref	m	0.9
Nominal mechanical power	Pn	MW	4.5
Specific speed number	Nq	-	54
Inertia of rotating mass	J_{tot}	$kg \cdot m^2$	535
Mechanical time constant	τ_m	s	1.3

3. Optimization method

3.1. Optimization approaches

The optimization process aims to obtain optimal trajectories for the Francis pump-turbine start-up sequence described by the design parameters allowing single or multi-objective optimization. Several approaches are available for solving engineering complex real-word problems, therefore heuristic genetic algorithms are considered as robust methods and commonly outperform conventional methods [12], [14], [15]. The objective functions evaluated with the SIMSEN physically-based model are derived from the non-linear behaviour of the pressure fluctuations of the hydraulic transient simulation. In this study, the commercial MATLAB toolbox were used to perform the single and multi-objective optimization [13]. The genetic algorithm solvers called GA and GAMULTIOBJ provide an effective global search in complex multi-objective optimization [14] and limit the local minima traps using the natural evolutionary principle. The genetic algorithm population-based starts with an initial population of solutions and then the population evolves with two main operators, the crossover and the mutation according to their fitness values. The crossover operator is used to combine the information of parents to generate new offspring and the mutation operator is used to insert random into the sampled populations. The fitness value of an individual, corresponding to the objective function value, determines the probability of its selection for the next generation. The algorithm used in this study is detailed in the MATLAB Global Optimisation toolbox [13].

The optimization approach is described in Figure 2. There are two distinct general approaches to perform either single objective optimization or multi-objective optimization. One is to combine the individual objective functions into a single function with the weighted multi-objective sum approach (WMA) and the second is to determine a Pareto optimal solution set called multi-objective genetic algorithm (MOGA). These two distinct optimization process exchange information with the hydraulic SIMSEN numerical model that is simulated to evaluate and assign the fitness value for the different objective functions. If the stopping criterion is satisfied, the optimization process terminate the search and return the final parameters describing the optimized trajectory of the start-up, otherwise, the iterations continue. In our specific case, WMA is used to perform single-objective optimization to find the reference optimal solutions for each single objective function and allowing their normalization by their best values. The normalization of each objective function is described in Figure 4, according to the fitness initial value (f^0) and the optimal fitness value (f^{best}) obtained by the optimization process. MOGA process aims to determine a Pareto front set of solutions that are non-dominated with the respect to each objective functions considered in the optimization process. The Pareto optimization approach is often preferred to single solution as WMA because the final solution of the decision-maker is often a trade-off based on well-known experiences and others operating constraints depending on the specificities of the hydropower plant.

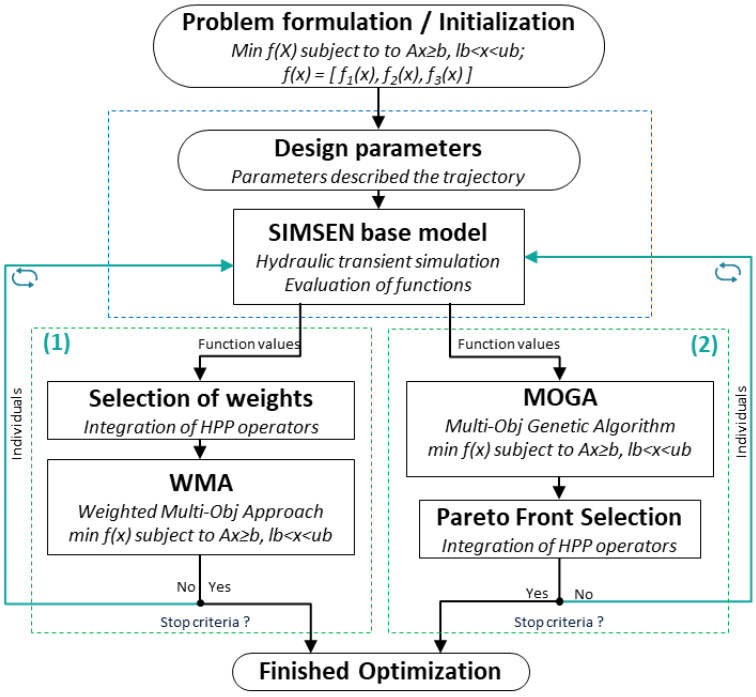

Figure 2: Methodology of the turbine start-up optimization.

3.2. Simulation based parameterization

The evaluation of the functions during the optimization process is performed with a numerical model of the Z'Mutt PSP, using the SIMSEN software [7]. The model has been implemented, calibrated and validated with comparison between measurements and simulations of transient events such as pump mode emergency shutdowns with different operating configurations of units. The model includes the complete hydraulic circuit comprising reservoirs, pipes, valves and the five units U1-U5. The simulation start-up sequence is driven with rotational speed and guide vanes parameters to reach the power set point. This control strategy has been tested and validated previously, see [8].

The start-up trajectory is defined with 20 parameters (see Table *2*). These decision parameters are part of the solution space of the optimization problem and are modified during the iteration of optimization process. Figure 3 shows the trajectory either in the time domain or in the N11-Q11 frame characteristic of the hydraulic turbine defined as the speed factor $N11 = n\,D/\sqrt{H}$ and the discharge factor $Q11 = Q/(D^2\sqrt{H})$. The parameters are the unit speed factor (N11), the guide vanes opening (y_i), the time (dt_i) passing between each point (P_i), the delay between the beginning of the guide vanes opening and the unit speed factor (dt_{yN}) and finally the duration of the whole sequence (t_{final}).

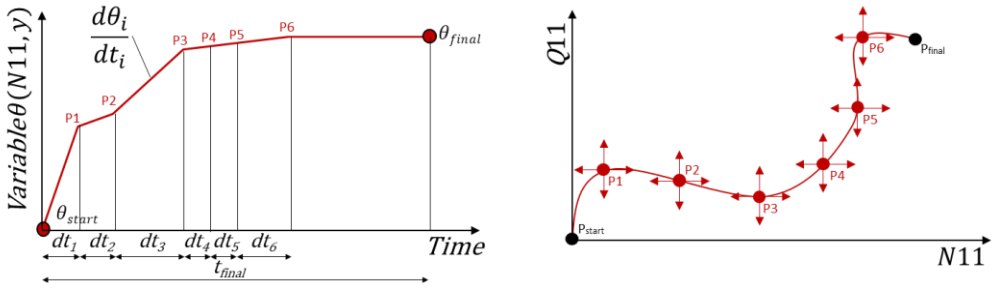

Figure 3: Parameterisation description of the start-up trajectory. Trajectory in time domain as function of speed factor, guide vanes opening and time vector (left). Trajectory in N11-Q11 frame bounded by starting point (standstill) and operating set point (BEP).

Table 2 summarizes the different decision parameters of scalar or vector type, forming the vector to be optimized and describing the trajectory of the turbine start-up sequence. The maximal interval of each decision parameters has to be determined, respecting the constraints, to reduce and restrict the search space of the problem. The bounds are defined according to the set point to be reached at the end of the sequence in terms of guide vanes opening and synchronous rotational speed. The minimum time limit for the duration is the allowing the fastest allowed sequence with respect to the GVO and rotational speed safety rates, and the maximum value of duration is arbitrary but allows to strongly reduce the pressure variation in terms of penstock fatigue while keeping fast start-up sequences.

Table 2: Decision parameters of the optimization with the bounds.

Definition of parameters	**Units**	**Parameters (scalar/vector)**	**Bounds**
Unit speed factor vector ($N11_i$)	[min^{-1}]	$\vec{\boldsymbol{x}}_{\boldsymbol{1}} = [N_1, N_2, \dots, N_6]$	$0 \leq N11_i \leq 88.04$
Guide-vanes opening vector (y_i)	[%]	$\vec{\boldsymbol{x}}_{\boldsymbol{2}} = [y_1, y_2, \dots, y_6]$	$0 \leq y_i \leq 0.97$
Time vector (dt_i)	[s]	$\vec{\boldsymbol{x}}_{\boldsymbol{3}} = [dt_1, dt_2, \dots, dt_6]$	$0 \leq dt_i \leq 22$
Delay between Y and N11 (dt_{yN})	[s]	$\boldsymbol{x_4} = dt_{yN}$	$0 \leq dt_{yN} \leq 2$
Duration of sequence (t_{final})	[s]	$\boldsymbol{x_5} = t_{final}$	$12.16 \leq t_{final} \leq 22$
Trajectory description ($\vec{\boldsymbol{x}}$)		$\vec{\boldsymbol{x}} = [\vec{\boldsymbol{x}}_{\boldsymbol{1}}, \vec{\boldsymbol{x}}_{\boldsymbol{2}}, \vec{\boldsymbol{x}}_{\boldsymbol{3}}, \boldsymbol{x_4}, \boldsymbol{x_5}]$	

The equality constraints of the optimization problem are imposed by the system itself and the components of the numerical simulation from the SIMSEN model. However, inequality constraints have to be imposed according to the safety and operability requirements. A safety threshold for turbine start-up is the guide vane opening rate to avoid severe transient pressure variation. These safety constraints, expressed as $Ax \leq b$, are the following : the maximum rotational speed rate (min^{-1}/s), the maximum guide vanes opening rate (%/s) and the positive incremental of the rotational speed.

3.3. Objective functions

To evaluate the simulated trajectories, it is required to set up objective functions able to quantify the fitness value of the turbine start-up sequence. This value must be described by a scalar to be minimized it. In our study, three main objective functions have been defined: the integration of the efficiency characteristic over time, the integration of the runner damage rate over time, the fatigue generated on the penstock. An additionally constraint function, used as penalty, is defined as the positive electromagnetic torque traduced by energy consumption during the start-up sequence. Figure 4 describe the different objective functions considered in the evaluation of the start-up sequence.

The efficiency function's aims to find the trajectory passing through the local best operating point (BEP tracking) to reduce flow disturbances in the runner and minimize water losses. The runner damage function's aims to minimize the runner's partial damage induced by the start-up sequence. The damage hill-chart has been deduced from one-way coupled FSI simulations using full CFD and FEM models of the pump-turbine, see [9]. The fatigue damage induced on the runner structure by the unsteady pressure fields is expresses in form of a standardized damage rate based on the stress-life approach as detailed in [9]. The penstock fatigue function's minimize the penstock pipe wall stress variation induced by the pressure fluctuations in the hydraulic scheme during the transient events, as mentioned in [10]. The cumulative damage on the penstock segments is computed with the static pressure evaluated at each time step of the simulation thanks to the transient SIMSEN model. Once the static pressure is converted into a stress (σ) with the Hoop stress equation $\Delta\sigma = \Delta p \cdot D/2e$, rain flow counting algorithm is applied to identify the stress cycles (amplitudes and cycle counts). Then cumulative damage is calculated using Palmgren-Miner's rule in accordance with BS7910 standard [11] as follows:

$$DT = \sum_i \left(\frac{n_i}{N_k} \left(\frac{\sigma_i}{\sigma_f} \right)^m \right) \quad (1)$$

with DT the damage tally, n_i the the number of cycles accumulated, N_k the endurance limit number of cycles to failure at $2e^6$ cycles, σ_i the stress range, σ_f the corresponding endurance limit stress range at $2e^6$ cycles and the exponent m related to the type of weld between the pipe segments.

Finally, all these three main objective functions are described in Figure 4. They are minimized in the optimization process either by using the weighted multi-objective sum approach or by performing a Pareto front trade-off of these objective functions.

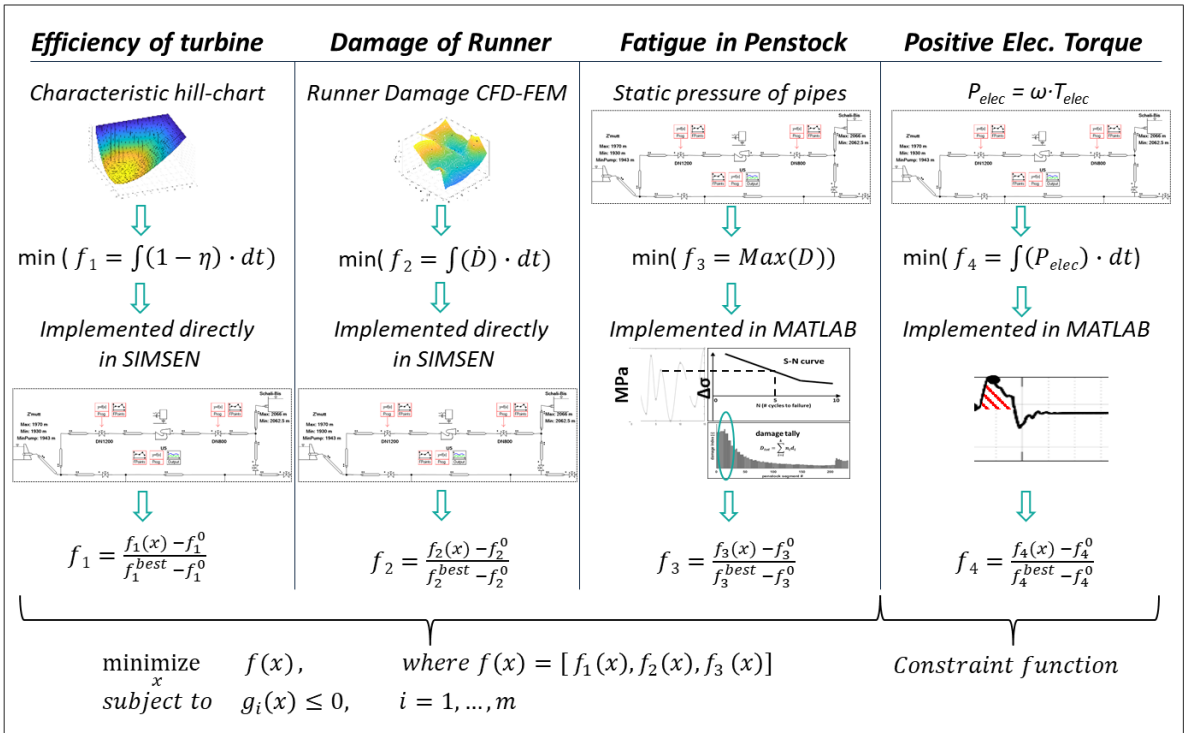

Figure 4: Description of the objective functions and their normalizations.

4. Optimization results

4.1. Evaluation of reference start-up sequences

The turbine start-up sequence with FSFC allows to avoid the damaging speed no load (SNL) area during synchronization to the grid. To evaluate the optimal sequences derived from optimization process, the standard fixed-speed start-up (SFS) and a linear variable-speed start-up (LVS) are evaluated by computing the objective functions. The two references operating point trajectories in the frame N11-Q11 and the transient results in time domain for both fixed-speed and linear variable-speed strategies are shown in Figure 5. Significant differences between the two sequences are noticeable such as the time duration of the sequence to reach the operating point and the synchronization to the power grid. For the standard fixed-speed sequence, the power set point is reached after 35 s which is already considered very efficient for a fixed-speed technology, since the synchronization itself could last than 1 minute. The speed regulator drives the guide vanes opening to stabilize the turbine at SNL condition during 15 s to perform the synchronization with the power grid. Then, once the unit is connected, the output power is increased to reach the set point.

However, with the FSFC, the unit is initially connected to the power grid when the unit is at standstill with closed guide vanes. To start the unit, the guide vanes are opened according to the safety maneuvering time and the rate of change of rotational speed is defined accordingly. The variable-speed start-up avoids the SNL area to mitigate unsteady flow conditions.

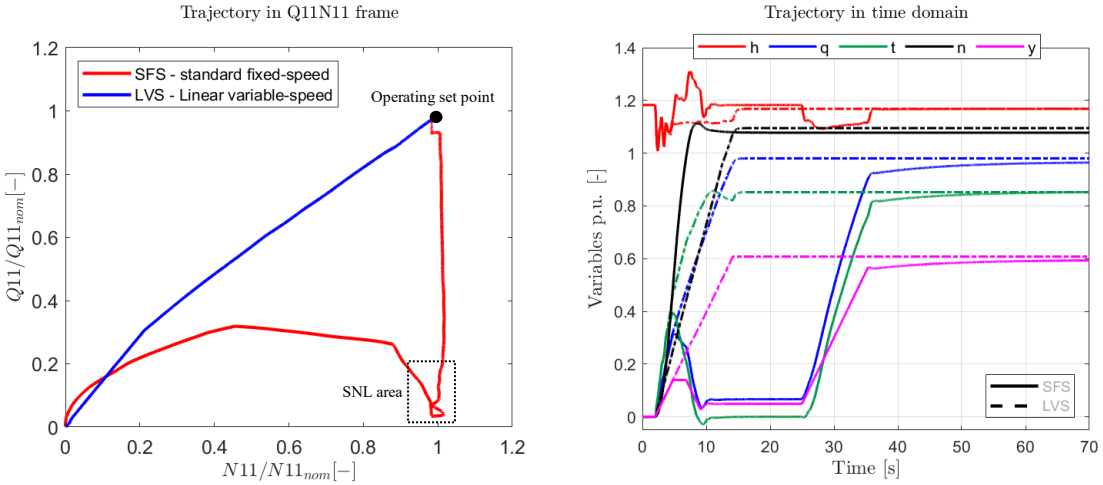

Figure 5: Trajectories of SFS and LVS start-ups in N11-Q11 frame (left) and in transient time domain (right: head h, discharge q, mechanical torque t, rotational speed n, guide vane opening y).

The results of the evaluation of objective functions (f_n) of the SFS and LVS start-up sequences are summarized in Table 3. For the efficiency tracking, the objective function value is around 5 times higher for the SFS compared to LVS sequence caused mainly by the time spend in the SNL condition. For the runner damage, the SFS start-up is 3 times more impactful for the runner than the LVS start-up. Indeed, the SNL area causes instabilities in flow pattern and therefore additional damage on runner are observed thanks to the CFD and FEM analysis. For the penstock fatigue, the LVS start-up reduced by 3 times the damage induced compared to the SFS start-up. The energy consumption during the sequence for the two start-up strategies are negligible, around 0 kWh. This energy penalty function allows to compute the power absorption peak consumed from the network knowing that the maximum allowed power absorption is 5% of the nominal power.

Table 3: Evaluation of functions for the standard fixed-speed and linear variable-speed start-up.

	Standard fixed-speed	**Linear variable-speed**
Objective functions (f_n)	**f_{SFS}**	**f_{LVS}**
Efficiency BEP tracking (f_1)	22.3	4.6
Runner damage (f_2)	81.7	29.6
Penstock fatigue (f_3)	2.2e-07	7.4e-08

4.2. Optimization results of single objective function

The optimization of each single objective function allows to get the best-trajectory for each of them and allows to extract the main trends of the different start-up sequences according to the individual objective function. It enables to validate the genetic algorithm using the well-known reference to obtain mainly for the efficiency BEP tracking and the runner damage based on the hill-charts. For the penstock fatigue, it's hard to know the trend of the reference trajectory because the function is highly non-linear. Moreover, these curves also help to have reference trajectories for the multi-objective optimization. To check the accuracy of the genetic algorithm, as mentioned previously, problems are compared to the well-known functions (visual check) and hypervolume is checked to be confident of the convergence using a population size of 200 individuals and the GA solver was run for 250 generations.

The three optimal trajectories for each function are shown in Figure 6 and they are represented in the N11-Q11 frame as well as in the time domain. The optimized trajectory of the efficiency function tends to follow the local best operating point while reaching the operating point as fast as possible. The optimized start-up for the runner damage finds a trajectory in N11-Q11 avoiding high damage by passing through the valley in the runner damage hill-chart. The runner damage map is plotted in logarithm scale in order to fully observe the variations of the damage amplitude. However, to be more realistic in the multi-objective optimization, the damage is applied as absolute values. The optimized trajectory of the penstock fatigue function tends to extend the time duration of the sequence by increasing guide vanes opening rate. As the function is only well-resolved by transient simulation, there is no visual hill-chart to validate the trajectory. However, in transient time domain, the aim is to minimize the pressure fluctuations represented by the head (h) in Figure 6.

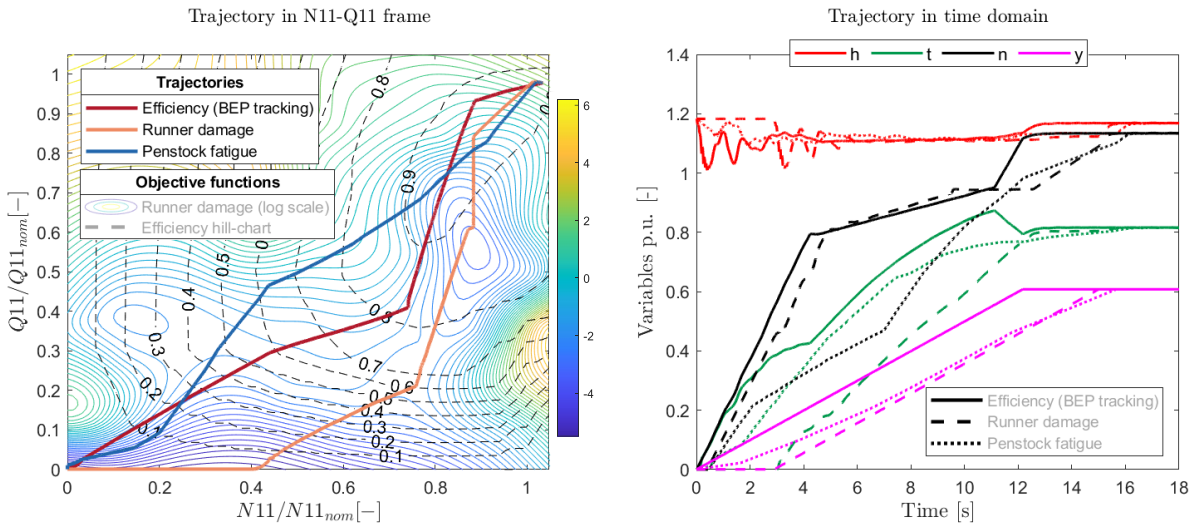

Figure 6: Start-up trajectories of optimal single objective function in Q11-N11 frame (left) and in transient time domain (right: head h, mechanical torque t, rotational speed n, guide vane opening y).

Table 4 shows the objective function values of each single optimal start-up as function of the reference start-ups (f_{ref}/f_n) allowing them to be compared as a factor. The efficiency function optimization finds a trajectory that improve respectively the f_1 by 7.7 and 1.6 compared to the SFS and LVS start-up. The runner damage optimized start-up improve respectively the f_2 by 7.7 and 2.8 compared to the SFS and LVS. It means that the runner damage is reduced by these factors as the optimization process is to minimize the f_2. The penstock fatigue optimized start-up improve respectively the f_3 by 49.5 and 16.5 compared to the SFS and LVS. It means the penstock fatigue is mitigated by the optimization process. The positive electromagnetic constraint function avoids having a start-up where the power absorption is greater than 5% of the nominal power. In the case of the runner damage optimized start-up, the power absorption is around 4.8% of the nominal power corresponding of 0.24 kWh. The duration of the optimized start-ups are also shown in Table 4. The overall trend is to have a relatively fast start-up between 12 and 16 seconds.

Table 4: Results of single objective function (f_n) optimization comparted to SFS and LVS references.

Objective functions (f_n)	**Start-up duration**	**f_{SFS}/f_n**	**f_{LVS}/f_n**
Efficiency BEP tracking (f_1)	~ 12 s	7.7	1.6
Runner damage (f_2)	~ 15 s	7.7	2.8
Penstock fatigue (f_3)	~16 s	49.5	16.5

4.3. Optimization with multi-objective Pareto approach

The Pareto-optimal front is obtained for the three objective functions with the non-dominate sorting genetic algorithm of MATLAB using a population of 250 individuals and a crossing probability of 0.6 running for 100 generations. Figure 7 (a) shows the tree-dimensional Pareto front of efficiency, runner damage and penstock fatigue functions. Figure 7 (b)-(d) display the two-dimensional Pareto fronts of the target pairs keeping the information of the 3rd function with color map. Four representative points are selected in the non-dominating solutions. The points A-B-C represents the feasible non-dominated extreme solution of each objective functions, respectively the efficiency (A), the runner damage (B) and the penstock fatigue (C). The point D represent a selected trad-off in the non-dominating solutions according to mitigate as well as the runner damage and the penstock fatigue.

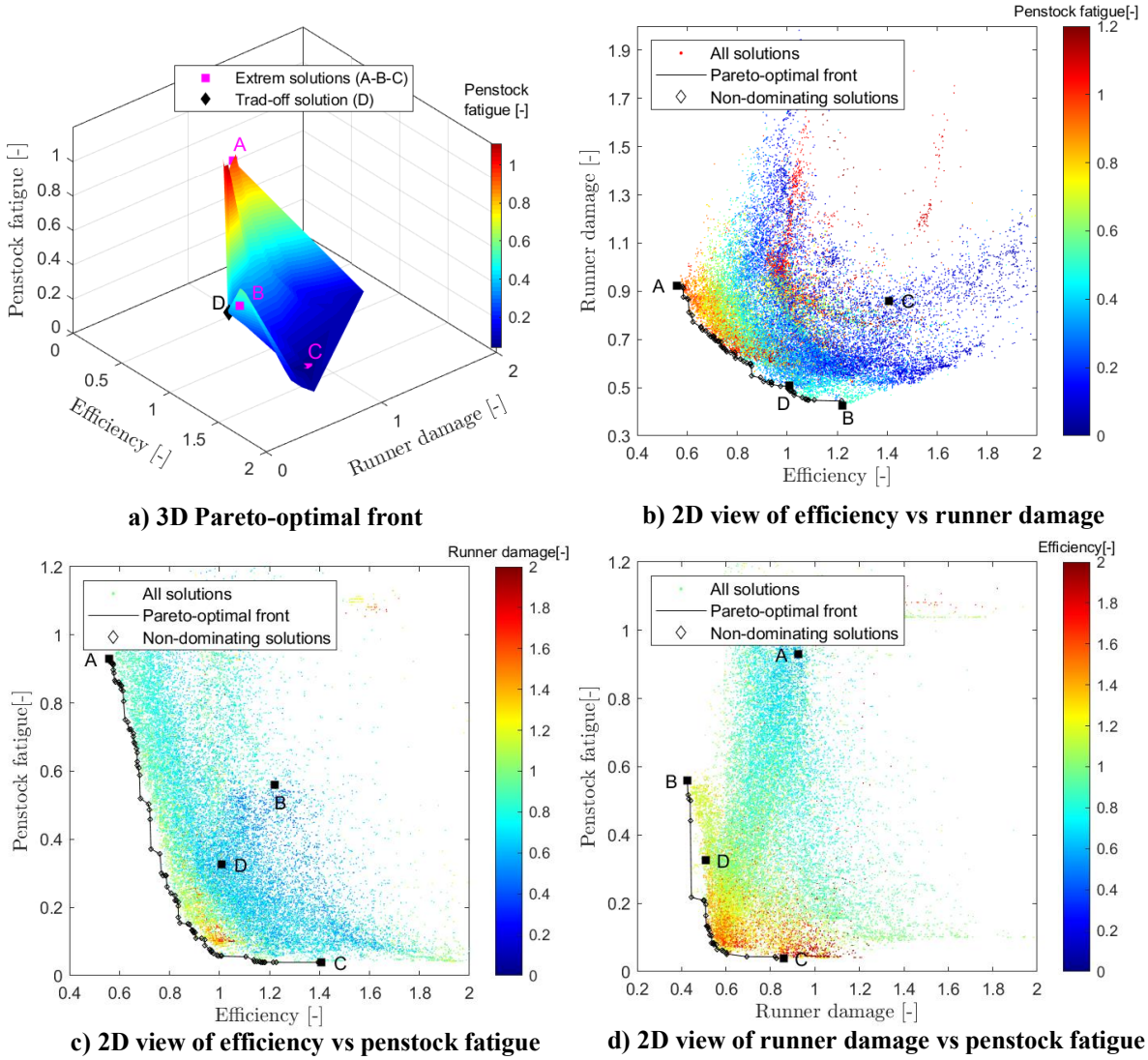

a) 3D Pareto-optimal front

b) 2D view of efficiency vs runner damage

c) 2D view of efficiency vs penstock fatigue

d) 2D view of runner damage vs penstock fatigue

Figure 7: Results of Pareto front of efficiency, runner damage and penstock fatigue for the start-up.

Table 5 shows the objective function values (f_n) of each selected points A-D. The results are referred to the SFS and LVS start-ups (f_{ref}/f_n) allowing them to be compared as a factor. The A-C trajectories show an improvement in their target functions. However, this improvement is slightly less significant when the single objective function optimization are performed. The trajectory D allows a compromise between the runner damage and the penstock fatigue, respectively by improving the $f_{2\text{-}3}$ by 3.6 and by 8.3

compared to SFS. The benefits are less significant compared to the LVS start-up. The trade-off trajectory D improves respectively $f_{2\text{-}3}$ by 1.3 and by 2.8 the runner damage and the penstock fatigue compared to the LVS start-up.

Table 5: Results of objective functions (f_n) compared to the reference sequences for selected points.

	Efficiency BEP tracking (f_1)		Runner damage (f_2)		Penstock fatigue (f_3)	
	f_{SFS}/f_i	**f_{LVS}/f_n**	**f_{SFS}/f_n**	**f_{LVS}/f_n**	**f_{SFS}/f_n**	**f_{LVS}/f_n**
Point A	**5.8**	**1.2**	2.5	0.9	3.4	1.1
Point B	4.5	0.9	**4.0**	**1.4**	5.3	1.8
Point C	4.2	0.9	2.6	0.9	**26.5**	**8.8**
Point D	4.8	1.0	**3.6**	1.3	**8.3**	2.8

Figure 8 compares the single optimized start-ups to the selected trade-off trajectory D in N11-Q11 frame and in transient time domain. In the N11-Q11 frame, the trajectory D feature similar pattern to the penstock fatigue function. One reason is that the absolute runner damage function has only very minor variation of amplitude on the most operating points compared to the logarithmic amplitude used in single objective function validation. For a more realistic damage on the runner, it is more interesting to take into account the absolute values. In the transient time domain, the start-up D begins with a slowly GVO ramp to avoid pressure fluctuations. The rotational speed is quiet similar of a linear trend with an attenuation ramp in the middle and a faster ramp at the end. The trade-off start-up consume negligible energy well below the allowed power absorption of 5% of the nominal power.

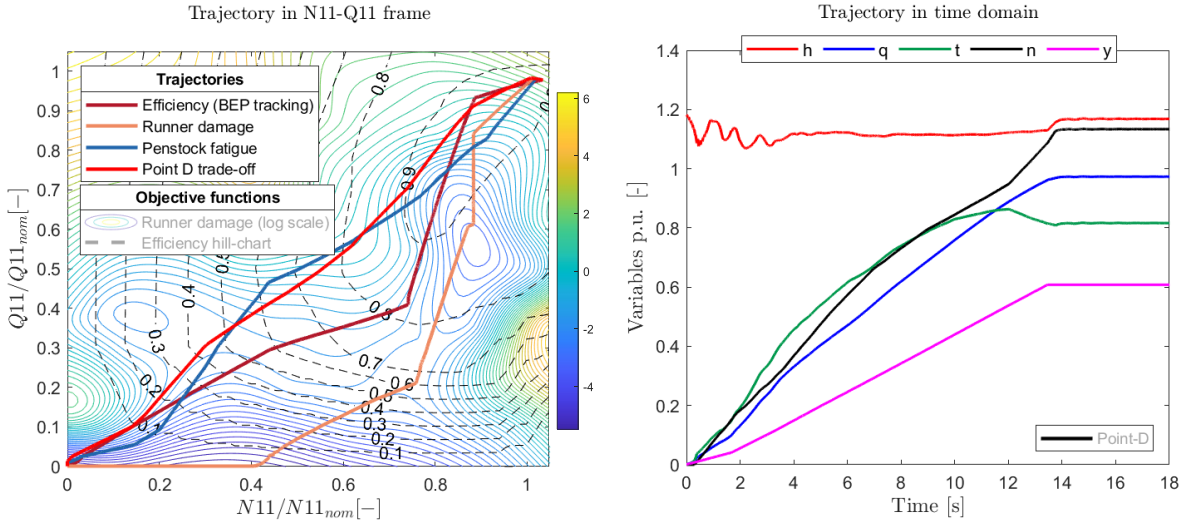

Figure 8: Start-up trajectories of selected A-D points in Q11-N11 frame (left) and the point D trade-off in transient domain (right: head h, discharge q, torque t, rotational speed n, guide vane opening y).

5. Conclusion

Optimization of 1D transient start-up sequence of reversible Francis pump-turbine equipped with FSFC have been performed and compared to a standard fixed-speed and linear variable-speed start-up. Three major objective functions have been taken into account in the optimization as the efficiency BEP tracking, the runner damage from CFD and FEM analysis and the penstock fatigue. The single objective optimization show that the efficiency target and runner damage tend to have similar trajectories in the N11-Q11 frame. Following the BEP tracking trajectory allows to strongly decrease the disturbances on the flow into the runner. But some differences have been observed in time domain as the delay between

the guide vanes opening and the rotational speed. Furthermore, the optimized penstock fatigue function has distinct trend compared to others in term of duration and guide vanes opening rates limitation to mitigate the pressure fluctuations at the beginning of the sequence. The benefits of the variable-speed technology compared to the conventional fixed-speed technology is significant, respectively by a factor of 7.7 for the runner damage and by 49.5 for the penstock fatigue. Furthermore, this study have shown that the linear variable-speed start-up equipped with FSFC has already significant mitigation compared to the conventional fixed-speed technology. Finally, the benefits on the runner damage and on the penstock fatigue of variable-speed technology would allow more numerous start and stop transient sequences and thus increase the flexibility of the unit. As perspectives, this approach could be applied to others transient sequences such as the stop and the transition from pumping mode to turbine mode.

6. Acknowledgements

The Hydropower Extending Power System Flexibility (XFLEX HYDRO) project has received funding from the European Union's Horizon 2020 research and innovation programme under grant agreement No 857832. The authors would like to thank CKD Blansko, Hydro Exploitation SA and Alpiq SA for their collaboration and support.

References

[1] https://xflexhydro.net/
[2] T. Kuwabara, A. Shibuya, H. Furuta, E. Kita, K. Mitsuhashi, Design and Dynamic Response Characteristics of 400 MW Adjustable Speed Pumped Storage Unit for Ohkawachi Power Station, IEEE Transactions on Energy Conversion, Vol. 11, Issue 2, pp. 376-384, June 1996.
[3] J. Löfflad, M. Eissner, Lifetime assessment and plant operation optimization based on geometry scan and strain gauge testing – START/STOP optimization, 10th International conference on hydraulic efficiency measurements, Itajuba, Brazil, 2014.
[4] V. Hasmatuchi, J. Decaix, M. Titzschkau, O. Pacot, C. Münch-Alligné, Detection of harsh operating conditions on a Francis prototype based on in-situ non-intrusive measurements, Proceedings of Hydro 2019, Porto, Portugal.
[5] M. Gagnon, J. Nicolle, On variations in turbine runner dynamic behaviours observed within a given facility, 2019 IOP Conf. Ser.: Earth Environ. Sci. 405 012005
[6] C. Nicolet, O. Braun, N. Ruchonnet, A. Béguin, F. Avellan, Full Size Frequency Converter for Fast Francis Pump-Turbine Operating Mode Transition, Proceedings of HYDROVISION International 2016, July 26-29, 2016, Minneapolis Convention Center, Minneapolis, USA.
[7] C. Nicolet, 2007, Hydroacoustic modelling and numerical simulation of unsteady operation of hydroelectric systems, EPFL, Thesis n° 3751.
[8] S. Alligné, et al., Turbine mode start-up simulation of a FSFC variable speed pump-turbine prototype – Part I :1D simulation, Proceedings of IAHR 2020, Lausanne, Switzerland.
[9] D. Biner, et al., Numerical fatigue damage analysis of a variable speed Francis pump-turbine during start-up in generating mode, Proceedings of IAHR 2022, Trondheim, Norway.
[10] M. Dreyer, et al., Digital clone for penstock fatigue monitoring, Proceedding of IAHR 2019, Stuttgart, Germany.
[11] BS 7910 2013 Guide to methods for assessing the acceptability of flaws in metallic structures.
[12] Koziel, S., Yang, X. S. Computational Optimization, Methods and Algorithms, 2011, DOI: 10.1007/978-3-642-20859-1-2.
[13] The MathWorks I. Global Optimization Toolbox. Natick, Massachusetts, United State; 2019. Available from: https://www.mathworks.com/help/gads/
[14] Jones DF, Mirrazavi SK, Tamiz M. Multiobjective meta-heuristics: an overview of the current state-of-the-art. Eur J Oper Res 2002;137(1):1–9.
[15] A. Konak, et al., Multi-objective optimization using genetic algorithms: a tutorial, Reliab. Eng. Syst. Saf. 91 (2006) 992–1007, https://doi.org/10.1016/j.ress.2005.11.018.